This article has been accepted for publication in IEEE/OSA Journal of Lightwave Technology. This is the author's version which has not been fully edited and content may change prior to final publication. Citation information: DOI 10.1109/JLT.2022.3199022

Static Beam Steering by Applying Metasurfaces on Photonic-Crystal Surface-Emitting Lasers

*Lih-Ren Chen, Chia-Jui Chang, Kuo-Bin Hong, Wei-Chih Weng, Bing-Hong Chuang, Yao-Wei Huang, and Tien-Chang Lu**

***Abstract*—Photonic-crystal surface-emitting laser (PCSEL) holds promise for laser beam with high efficacy while retain the small divergence angle, being now all the rage as laser source in modern opto-electronic technologies to replace edge emitting lasers and vertical-cavity surface-emitting lasers (VCSELs). Arbitrary beam shaping and deflection of VCSELs with ultra-thin flat optics, aka metasurfaces, has recently demonstrated, making possibility to realize a compact system in many technologies. However, the large divergence angle and limited output power at single fundamental mode of the VCSEL limits its application. Here, we report the static steering of laser beam with high efficiency and near 1º divergence angle by shining the laser beam of the PCSEL through the metasurface array placed on top. The small divergence angle is contributed from PCSEL. On the other hand, the metasurface array offers the higher efficiency beam deflection, without considering additional collimating or focusing. This provides highly flexible platform and is capable to manipulate the laser emission through the design of the metasurfaces and the PCSELs. Moreover, the beam proprieties can be further modified for specific application through the metasurfaces. The integration of metasurface with PCSEL provides the compact and collimated laser source, promising more accurate generation of versatile laser sources on demand for automotive ultra-compact light detection and ranging (LiDAR), depth sensing, optical communication, etc.**

***Index Terms*—photonic-crystal surface-emitting laser, metasurface, high power, small divergence, beam deflection.**

I. Introduction

The applications of light detection and ranging (Lidar) and three-dimensional (3D) sensing technologies on the autonomous vehicles and mobile devices are soaring rapidly in recent years. Among those systems, semiconductor lasers and silicon photonics technologies are indispensable to maintain the performance in miniature device footprint. [1-4] The laser beams are spatially modulated to be incident onto the detected object and the reflected beams are collected to present the contour through specific algorithm. Take Lidar systems for instance, approaches for manipulation of laser beams, such as optical phase array (OPA) through silicon photonics technologies, reflective mirror through micro electro mechanical systems (MEMs), and active devices using reconfigurable metasurfaces are applied to replace the traditional optomechanical parts.[5-8] For the generation of structured beam pattern, a laser beam was shaped as rectangular through a diffusor and followed by passing through a diffractive optical element (DOE) to produce the beam pattern. The laser sources typically applied in these systems are edge emitting lasers or vertical-cavity surface-emitting laser (VCSEL) arrays for which the large beam divergences and the limited output power for single mode operation complicates the design and restricts its applications.[9] Recently, photonic-crystal surface-emitting lasers (PCSELs) were demonstrated to exhibit advantageous features of high output power, single mode operation, and small divergence angle which enables the direct application on the above-mentioned applications.[10-13] Moreover, direct modulation of the output beam angle has been demonstrated on PCSELs, which facilities the further reduction of the system footprint[3, 14-20]. R. Sakata et, al. realized the beam steering of the PCSEL via the periodical modulation of the shape and position of the photonic crystal (PC) to generate a crystal momentum that deflects the beam direction.[3] The far-field divergence was kept around 1º as the regular PCSELs, which enables direct application without focusing or collimating lenses. In our previous report, the integration of the diffractive elements on the PCSELs has been presented to control the beam direction[16, 21]. In this study, our attempt is to apply the metasurfaces for beam deflection with refined beam shape and the efficacy on the PCSELs.

Metasurfaces, consisted of subwavelength nano-scaled structures, has been extensively applied for manipulating or shaping the wave front with high efficacy through a thin layer.[22-29] Moreover, the generation of laser beams with high order orbital angular momentum (OAM) through metasurfaces has been reported. [30-32] The integration of PCSELs with metasurfaces are expected to combine the advantages of these two devices and deliver many more kinds of versatile lasers in our concept. Through this approach, the laser properties on demand can be obtained directly without additional optical elements. In current status, the laser beam properties such as the deflection angle and beam divergence were investigated through the injection of the laser beam into the metasurfaces placed on top of the PCSEL. The directionally modulated laser beam via the metasurfaces was shown to preserve the feature of small divergence angle, and speckless captured by beam viewer. Such kind of laser performance is

This work has been financially supported in part by the Ministry of Science and Technology in TAIWAN under Contract No. MOST 110-2221-E-A49-058-MY3, MOST 110-2218-E-A49-012-MBK, and MOST 109-2627-M-008-001.

Lih-Ren Chen, Chia-Jui Chang, Kuo-Bin Hong, Wei-Chih Weng, Bing-Hong Chuang, Yao-Wei Huang, and Tien-Chang Lu are with the Department of Photonics and Institute of Electro-Optical Engineering, National Yang Ming Chiao Tung University, 1001 University Road, Hsinchu 30050, Taiwan. (phone: +886-3-5131234; fax: +886-3-571-6631; corresponding e-mail: timtclu@nycu.edu.tw).

This article has been accepted for publication in IEEE/OSA Journal of Lightwave Technology. This is the author's version which has not been fully edited and content may change prior to final publication. Citation information: DOI 10.1109/JLT.2022.3199022

promising for the application of 3D sensing and Lidar applications

II. Experimental

The PCSEL applied as a light source in this experiment was designed and fabricated, which was described in previous report. [33-35] Following will deliver the design and fabrication of the metasurfaces as well as the measurement setup.

A. *Design and fabrication of metasurfaces*

A supper cell of metasurface blazed grating (Fig. 1(a) right) is composed of several (≥ 3) meta-atoms. The meta-atom or building block of our metasurface blazed grating is design as 600-nm-tall circular GaAs nano-pillars on GaAs substrate (Fig. 2a left). Different phase shift can be imparted by changing the radius of the pillar and the center-to-center distances (in x-direction, Lx) of each pillar. The phase shift of the circular nano-pillars was numerical calculated with commercial finite element method (COMSOL). Fig. 2b and 2c shows the respective simulated transmitted phase and transmittance of nano-pillar versus different center-to-center distances and radius. We assume the incident light is from the bottom substrate with normal incidence. Therefore, the deflection angle of the beam passing through metasurface grating can be determined by

$$\theta = sin^{-1}\left(\frac{\lambda}{w}\right) \qquad (1)$$

where w, Θ, and λ represent the width of the supercell (in x-direction), deflection angle, and wavelength, respectively. To satisfy the required diffraction angle, e.g. 20°, the supercell periodicity should be 2778 nm. Therefore, we select six different nano-pillars (labeled on Fig. 1(b)) with appropriate phase difference and transmittance while the sum of their Lx satisfies the supercell periodicity and the higher diffraction efficiency is considered.

The metasurfaces were fabricated on the double side polished GaAs wafer in avoidance of scattering from the rough surface of the substrate. The e-beam lithography was applied to generate the pattern of the metasurfaces on poly methyl methacrylate (PMMA) which served as the photoresist as well as the mask for the following etching process. An inductively coupled plasma - reactive ion etching (ICP-RIE) process with chlorine-based reaction gas was carried out to etch off the unmasked GaAs to form the nanopillars. The pattern size of each nanopillar has been revised to compensate the variation of etching rate of different pillar size. The etching parameters was refined to maintain the steep side walls as shown in the right panel of Fig. 1(c). Fig. 1(c) shows the scanning electron microscope (SEM) image of one of our fabricated metasurface grating. The metasurface for each deflection angle designed and fabricated according to above method was evaluated for the performance.

1(a)

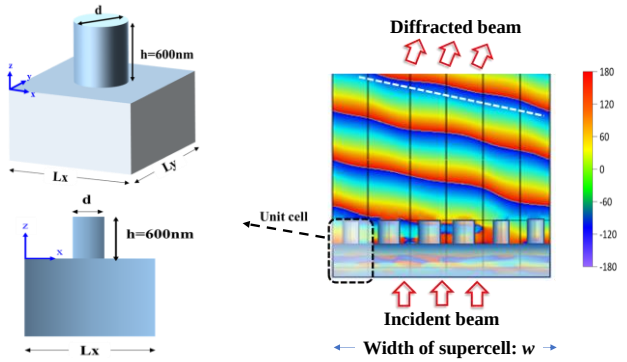

1(b)

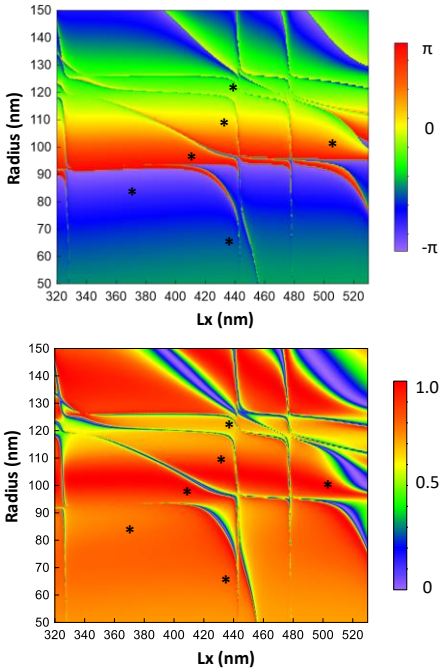

1(c)

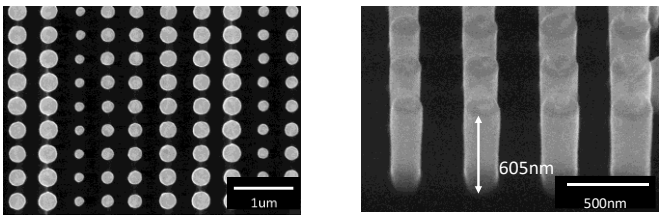

Figure 1. (a) The illustration of operation principle and design of metasurfaces. (b) The mapping diagram of the phase (left panel) and transmittance (right panel) with respect to the unite cell geometries. The asterisk on the diagram indicated the chosen unite cells to compose the metasurface. (c) The top view (left panel) and the inclined view (right panel) of the nanopillars through the SEM observation.

B. *The characterization of the deflected laser beam*

In this section, the measurement setup will be depicted. The metasurface of specific deflection angle was measured through the angle resolved electroluminescence (AREL) set as the schematic diagram shown in Fig. 2(a). The PCSEL was applied

as the light source and shined the metasurface placed atop. The signal was collected through a fiber with a varying polar angle at 0.1° step and the signal was collected by the photodiode.

We further assembled an array of 7 × 7 metasurfaces with variety deflection angles to demonstrate a squared pattern with deflection angle spanning in the range of ±20°. The OM picture of the array was displayed in left panel of Fig. 2(b). The metasurface array was placed on the sample holder at 10 *mm* height above the PCSEL, which was free to move parallelly relative to the PCSEL as shown in the schematic diagram shown in Fig. 2(b). The emitted laser beam covered approximately four metasurface patterns of the array and hence, laser beams with four deflected angles were collected on the beam viewer of each measurement. The metasurface array was moved with respective to the PCSEL to ensure all the deflected angles through the metasurface array were covered.

2(a)

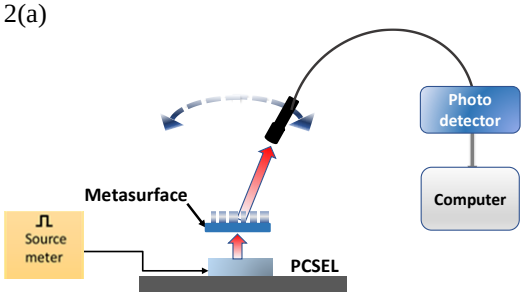

2(b)

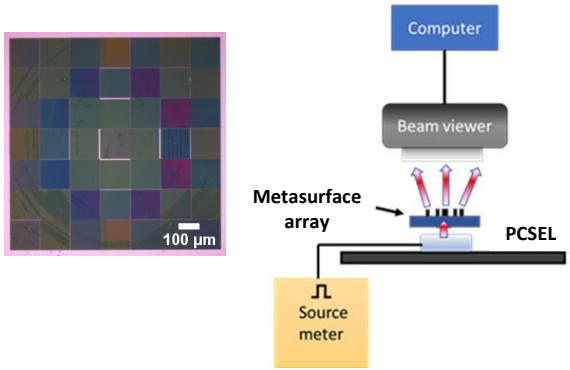

Figure 2. (a) Schematic illustration of AREL measurement of metasurface excited by PCSEL for specific deflection angle. (b) The OM picture of the top view of metasurfaces array (left panel). The measurement setup for the evaluation of the far field pattern of the electrically driven PCSEL device integrated with metasurface arrays (right panel).

III. Results and Discussion

A. PCSELs

Fig. 3(a) represents the light-current-voltage (L-I-V) characteristics and lasing spectrum measured at driving current of 1.2 × I_{th} of the PICSEL which ensures single lasing peak at 950 nm. The emission intensity taken near the threshold is uniformly distributed as indicated in the near field pattern shown on the upper panel of Fig. 3(b). The far field pattern shown on the lower panel Fig. 3(b) represents a single lasing mode with divergence angle as small as ~1° and laser beam quality factor (M^2) as good as 1.4. The uniformly single lateral lasing mode facilitates the fabrication of metasurface directly on the substrate of PCSEL in the future. The measured degree of polarization (DOP) in Fig. 3(c) is 79% owing to the PC geometry. Though the current metasurface is insensitive to the polarization, it has to take into consideration while using other sorts of metasurface design. The single mode and low divergence properties of the laser beam emitted from the PCSEL, benefited from the distributed feedback oscillation of large surface area, will be favorable for integration with metasurfaces.

3(a)

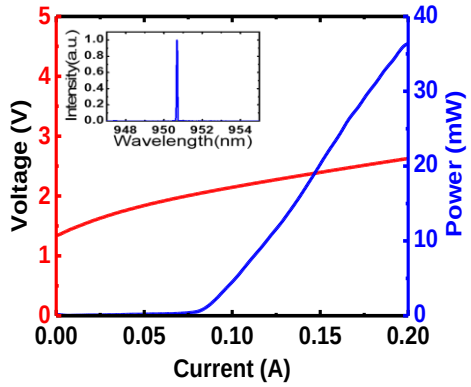

3(b) 3(c)

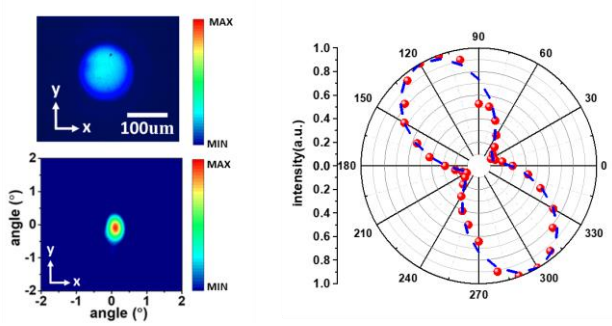

Figure 3. (a) The L-I-V curves and the lasing spectrum of the single PCSEL device. (b) the near field image (upper panel) and the far field pattern (lower panel) of the PCSEL. (c) the measured DOP.

B. Metasurfaces

Fig. 4 depicts four instances of the experimental results of the metasurfaces, where the upper and lower panel shows the polar plot of beam profiles and the SEM top view, respectively. The dimension of the fabricated metasurface matches well with the design value with overall deviation less than 5%, which results in the well side lobe supersession and low half width of the main peak. This indicates the metasurface effectively deflected the

This article has been accepted for publication in IEEE/OSA Journal of Lightwave Technology. This is the author's version which has not been fully edited and content may change prior to final publication. Citation information: DOI 10.1109/JLT.2022.3199022

laser beam and well preserve the small divergence angle of the PCSEL. Owing to the large area coherent emission of PCSEL, the design of the metasurface is simplified by utilizing plane wave incidence. Once we have confirmed that the performance of the metasurfaces met our requirement, the design and the fabrication process were applied on the metasurfaces array.

C. Metasurfaces array

The metasurfaces array was designed to project the laser beams for various deflection angles with projected wave vector depicted as Kx and Ky in Fig. 5(a) which corresponds to a square pattern in real space. The dummy metasurface consisted of equal-phase nanopillar was applied for the 0° deflection to normalize the transmittance of the metasurafces. Fig. 5(b) displays the far field emission pattern of this integrated device which is driven by the current pulse of 10μs and 10% duty cycle. The deflected laser beam was detected by the beam viewer as described in previous section. The data collected of each measurement was assembled in one frame as shown in Fig. 5(b). To ensure the deflection angle and the intensity, we move two patterns of metasurfaces array per step and keep two patterns

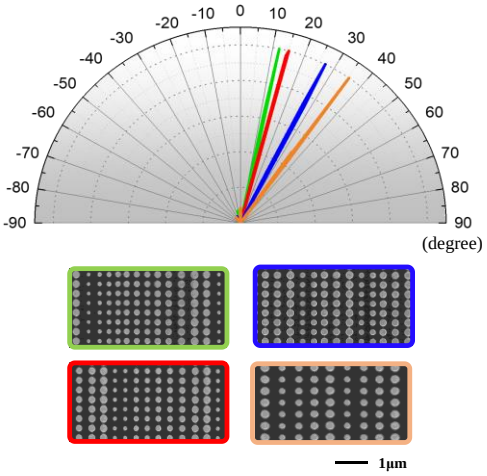

Figure 4. The polar plot of angle dependent spectrum of the four metasurface structures (upper panel) and the top view of the nanopillars through SEM measurement corresponding to each indicated color (lower panel).

overlapped. The deflection angles and the intensities of the two repeated patterns are applied for calibration of the other two patterns. The bright laser spot in contrast to the background detected by the beam viewer can be clearly observed at each designed deflection angle without any speckle. Such kind of light pattern will be promising for applications such as 3D sensing that a high signal to noise ratio will be expected. The divergence angle of the laser beam still maintains at ~1° after passing through the metasurface regardless of the deflection angle, which in accordance with previous measurement. This is advantageous for direct application without further beam shaping and focusing, which is expect to reduce the footprint of the whole system. From Fig. 5(b) we can notice the intensity of the laser spot is lower at deflection angle of 20° that we have not observed in the individual pattern. This resulted from the deviation of the height of nanopillars during the process that the photo resist for e-beam lithography was thicker around the edge of the sample during the spin coating process. The thicker photoresist leads the exposure condition deviated from our setting and hence a thin residual photo resist layer left to retard the etching of GaAs layer. The deviation of the geometries of the nano pillar led to incomplete 2 π phase coverage and hence reduced intensity. This can be avoided by the refinement of the process parameter or just simply using a larger piece of sample to prevent from the edge effect. In this study, we characterized the performance of the two devices independently and the two components were integrated to show the novel beam characteristics. For the next step, the fabrication of PCSEL with n side emission and the metasurfaces directly on the substrate will be fulfilled to further reduce the optical losses at the interfaces.

5(a)

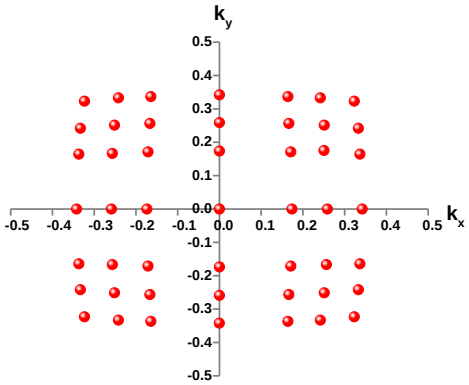

5(b)

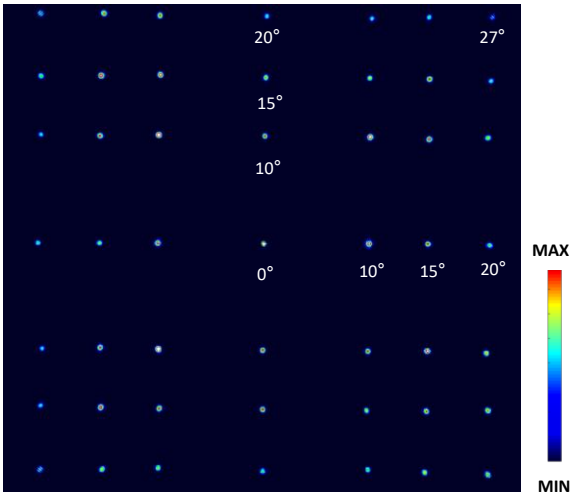

Figure 5. (a) The estimated deflection angles of the metasurfaces array represented in k space vector. (b) the measured far field pattern presented on the beam viewer.

IV. Conclusion

In this report, we demonstrated the deflection of emission angle of the PCSEL by the metasurface with high efficacy and fidelity. The inherent characteristics of the PCSEL that the small divergence angle due to the large area coherent oscillation is favorable for the design of metasurfaces without considering additional collimating or focusing. The deflected beam through the metasurfaces preserved the small beam divergence of the PCSEL which is advantageous for direct apply without beam shaping. The integration of metasurfaces with PCSELs shall pave the way for the versatile laser source for multiple functions with miniature device volume."

Acknowledgment

This work has been financially supported in part by the Ministry of Science and Technology in TAIWAN under Contract No. MOST 110-2221-E-A49-058-MY3, MOST 110-2218-E-A49-012-MBK, and MOST 109-2627-M-008-001. The authors would like to acknowledgment GIS Corp., Taiwan, LandMark Optoelectronics Corp., Taiwan, Nano Facility Center (NFC), Center for Nano Science and Technology (CNST) in NYCU, and also the Industrial Technology Research Institute (ITRI) for their technical support.

References

[1] M. Dummer *et al.*, "The role of VCSELs in 3D sensing and LiDAR," presented at the Optical Interconnects XXI, 2021.

[2] S. Wake *et al.*, "Optical system design and integration of the Global Ecosystem Dynamics Investigation Lidar," presented at the Infrared Remote Sensing and Instrumentation XXVII, 2019.

[3] R. Sakata *et al.*, "Dually modulated photonic crystals enabling high-power high-beam-quality two-dimensional beam scanning lasers," *Nat Commun*, vol. 11, no. 1, p. 3487, Jul 17 2020, doi: 10.1038/s41467-020-17092-w.

[4] B. Schwarz, "Mapping the world in 3D," *Nature Photonics*, vol. 4, no. 7, pp. 429-430, 2010, doi: 10.1038/nphoton.2010.148.

[5] C. V. Poulton *et al.*, "Coherent solid-state LIDAR with silicon photonic optical phased arrays," *Opt. Lett.*, vol. 42, no. 20, pp. 4091-4094, Oct 15 2017, doi: 10.1364/OL.42.004091.

[6] A. Yaacobi, J. Sun, M. Moresco, G. Leake, D. Coolbaugh, and M. R. Watts, "Integrated phased array for wide-angle beam steering," *Opt. Lett.*, vol. 39, no. 15, pp. 4575-8, Aug 1 2014, doi: 10.1364/OL.39.004575.

[7] D. Wang, C. Watkins, and H. Xie, "MEMS Mirrors for LiDAR: A review," *Micromachines (Basel)*, vol. 11, no. 5, Apr 27 2020, doi: 10.3390/mi11050456.

[8] P. C. Wu *et al.*, "Dynamic beam steering with all-dielectric electro-optic III-V multiple-quantum-well metasurfaces," *Nat Commun*, vol. 10, no. 1, p. 3654, Aug 13 2019, doi: 10.1038/s41467-019-11598-8.

[9] Y. Y. Xie *et al.*, "Metasurface-integrated vertical cavity surface-emitting lasers for programmable directional lasing emissions," *Nat Nanotechnol*, vol. 15, no. 2, pp. 125-130, Feb 2020, doi: 10.1038/s41565-019-0611-y.

[10] K. Hirose, Y. Liang, Y. Kurosaka, A. Watanabe, T. Sugiyama, and S. Noda, "Watt-class high-power, high-beam-quality photonic-crystal lasers," *Nature Photonics*, vol. 8, no. 5, pp. 406-411, 2014, doi: 10.1038/nphoton.2014.75.

[11] M. Yoshida *et al.*, "Double-lattice photonic-crystal resonators enabling high-brightness semiconductor lasers with symmetric narrow-divergence beams," *Nat Mater*, vol. 18, no. 2, pp. 121-128, Feb 2019, doi: 10.1038/s41563-018-0242-y.

[12] R. Morita, T. Inoue, M. De Zoysa, K. Ishizaki, and S. Noda, "Photonic-crystal lasers with two-dimensionally arranged gain and loss sections for high-peak-power short-pulse operation," *Nature Photonics*, vol. 15, no. 4, pp. 311-318, 2021, doi: 10.1038/s41566-021-00771-5.

[13] S.-C. Huang *et al.*, "Design of photonic crystal surface emitting lasers with indium-tin-oxide top claddings," *Appl. Phys. Lett.*, vol. 112, no. 6, 2018, doi: 10.1063/1.5016442.

[14] S. Noda, K. Kitamura, T. Okino, D. Yasuda, and Y. Tanaka, "Photonic-Crystal Surface-Emitting Lasers: Review and Introduction of Modulated-Photonic Crystals," *IEEE Journal of Selected Topics in Quantum Electronics*, vol. 23, no. 6, pp. 1-7, 2017, doi: 10.1109/jstqe.2017.2696883.

[15] L.-R. Chen, H.-L. Chiu, K.-B. Hong, and T.-C. Lu, "Low threshold current photonic crystal surface emitting lasers with beam modulation capability," presented at the Conference on Lasers and Electro-Optics, 2019.

[16] L. R. Chen, K. B. Hong, H. L. Chen, K. C. Huang, and T. C. Lu, "Vertically integrated diffractive gratings on photonic crystal surface emitting lasers," *Sci Rep*, vol. 11, no. 1, p. 2427, Jan 28 2021, doi: 10.1038/s41598-021-82194-4.

[17] J. Yang, D. Sell, and J. A. Fan, "Freeform Metagratings Based on Complex Light Scattering Dynamics for Extreme, High Efficiency Beam Steering," *Annalen der Physik*, vol. 530, no. 1, 2018, doi: 10.1002/andp.201700302.

[18] Y. W. Huang *et al.*, "Gate-Tunable Conducting Oxide Metasurfaces," *Nano Lett.*, vol. 16, no. 9, pp. 5319-25, Sep 14 2016, doi: 10.1021/acs.nanolett.6b00555.

[19] M. J. R. Heck, "Highly integrated optical phased arrays: photonic integrated circuits for optical beam shaping and beam steering," *Nanophotonics*, vol. 6, no. 1, pp. 93-107, 2017, doi: 10.1515/nanoph-2015-0152.

[20] T. Komljenovic, R. Helkey, L. Coldren, and J. E. Bowers, "Sparse aperiodic arrays for optical beam forming and LIDAR," *Opt. Express*, vol. 25, no. 3, pp. 2511-2528, Feb 6 2017, doi: 10.1364/OE.25.002511.

[21] H.-L. Chiu, K.-B. Hong, K.-C. Huang, and T.-C. Lu, "Photonic Crystal Surface Emitting Lasers with Naturally Formed Periodic ITO Structures," *ACS Photonics*, vol. 6, no. 3, pp. 684-690, 2019, doi: 10.1021/acsphotonics.8b01530.

[22] D. Lin, P. Fan, E. Hasman, and M. L. Brongersma, "Dielectric gradient metasurface optical elements," *Science*, vol. 345, no. 6194, pp. 298-302, Jul 18 2014, doi: 10.1126/science.1253213.

[23] A. Rahimzadegan *et al.*, "Beyond dipolar Huygens' metasurfaces for full-phase coverage and unity transmittance," *Nanophotonics*, vol. 9, no. 1, pp. 75-82, 2020, doi: 10.1515/nanoph-2019-0239.

[24] D. Lin *et al.*, "Polarization-independent metasurface lens employing the Pancharatnam-Berry phase," *Opt. Express*, vol. 26, no. 19, pp. 24835-24842, Sep 17 2018, doi: 10.1364/OE.26.024835.

[25] D. Sell, J. Yang, E. W. Wang, T. Phan, S. Doshay, and J. A. Fan, "Ultra-High-Efficiency Anomalous Refraction with Dielectric Metasurfaces," *ACS Photonics*, vol. 5, no. 6, pp. 2402-2407, 2018, doi: 10.1021/acsphotonics.8b00183.

[26] B. Li, W. Piyawattanametha, and Z. Qiu, "Metalens-Based Miniaturized Optical Systems," *Micromachines (Basel)*, vol. 10, no. 5, May 8 2019, doi: 10.3390/mi10050310.

[27] W. T. Chen, A. Y. Zhu, J. Sisler, Z. Bharwani, and F. Capasso, "A broadband achromatic polarization-insensitive metalens consisting of anisotropic nanostructures," *Nat Commun*, vol. 10, no. 1, p. 355, Jan 21 2019, doi: 10.1038/s41467-019-08305-y.

[28] W. T. Chen, A. Y. Zhu, and F. Capasso, "Flat optics with dispersion-engineered metasurfaces," *Nature Reviews Materials*, vol. 5, no. 8, pp. 604-620, 2020, doi: 10.1038/s41578-020-0203-3.

[29] Y. Ni, S. Chen, Y. Wang, Q. Tan, S. Xiao, and Y. Yang, "Metasurface for Structured Light Projection over 120 degrees Field of View," *Nano Lett.*, vol. 20, no. 9, pp. 6719-6724, Sep 9 2020, doi: 10.1021/acs.nanolett.0c02586.

[30] T. Stav *et al.*, "Quantum entanglement of the spin and orbital angular momentum of photons using metamaterials," *Science*, vol. 361, no. 6407, pp. 1101-1104, Sep 14 2018, doi: 10.1126/science.aat9042.

[31] H. Ren *et al.*, "Metasurface orbital angular momentum holography," *Nat Commun*, vol. 10, no. 1, p. 2986, Jul 19 2019, doi: 10.1038/s41467-019-11030-1.

[32] H. Sroor *et al.*, "High-purity orbital angular momentum states from a visible metasurface laser," *Nature Photonics*, vol. 14, no. 8, pp. 498-503, 2020, doi: 10.1038/s41566-020-0623-z.

[33] L. R. Chen, K. B. Hong, K. C. Huang, H. T. Yen, and T. C. Lu, "Improvement of output efficiency of p-face up photonic-crystal surface-emitting lasers," *Opt. Express*, vol. 29, no. 7, pp. 11293-11300, Mar 29 2021, doi: 10.1364/OE.421019.

[34] K.-B. Hong *et al.*, "Impact of Air-Hole on the Optical Performances of Epitaxially Regrown P-Side Up Photonic Crystal Surface-Emitting Lasers," *IEEE Journal of Selected Topics in Quantum Electronics*, vol. 28, no. 1, pp. 1-7, 2022, doi: 10.1109/jstqe.2021.3095961.

[35] L.-R. Chen, K.-B. Hong, K.-C. Huang, C.-L. Liu, W. Lin, and T.-C. Lu, "Study of an Epitaxial Regrowth Process by MOCVD for Photonic-Crystal Surface-Emitting Lasers," *Crystal Growth & Design*, vol. 21, no. 6, pp. 3521-3527, 2021, doi: 10.1021/acs.cgd.1c00280.